Study on A "Tactile Mirror" for Displaying Static Friction Sensation with Tactile Perception Feedback

Isao Fujimoto*, Yoji Yamada*, Takashi Maeno, Tetsuya Morizono* and Yoji Umetani*****

*Intelligent Robotics Laboratory, Toyota Technological Institute
2-12-1, Hisakata, Tenpaku-ku, Nagoya 468-8511, Japan
**Department of Mechanical Engineering, Keio University
3-14-1, Hiyoshi, Kohoku-ku, Yokohama 223-8522, Japan
***Intelligent Systems Laboratory Ltd.
4-8-11-207, Takanawa, Minato-ku Tokyo, 108-0074, Japan

Abstract

The goal of our study is development of a "tactile mirror" for displaying tactile perception information. A point of distinctive difference between a tactile mirror and conventional tactile displays is that a tactile mirror possesses a feedback mechanism for acquiring the contact state information on the finger pad concerning not force but tactile perception sensation. The primary development concerns human static friction sensation. First, a control method and the structure of a tactile mirror are described. Second, simulation results using FEM for contact analysis and a ANN(Artificial Neural Network) for generating feedback signals are shown. Finally, experiments demonstrating that providing a feedback component accomplish accurate display of static friction sensation with a conventional type of tactile displays.

1 Introduction

Recently, it is expected that tactile media will serve as the third important human interface after visual and auditory media. Particularly, studies on VR(Virtual Reality) are demanded for acquiring force and/or tactile display information that can be fed back to human masters' sides so that they can perceive physical constraints from their environment[1]. Several attempts have been made to display tactile perception sensation, such as deformation of human finger tips[2] in the shearing direction.

There are many studies of displaying tactile perception sensation. For example, Dimitrios *et al.* developed a set of tactile shape sensing and display system for teleoperated manipulation[3]. 6×4 arrays of SMA(Shape Memory Alloy)-driven pin elements cause human shape sensation in their development.

Due to advancement of computers, studies of realizing advanced tactile perception sensation display have been reported more recently. For example, Debus *et al.* presented the design and testing of a multi-channel vibrotactile display[5]. The device was tested in a manner of sensory substitution for conveying force information during a teleoperated peg insertion. Their results showed that the device was effective in reducing maximum forces during the insertion task. Richard *et al.* reported a state-of-the-art haptic interface in friction estimation and presented a method for rendering the friction based on a modified Karnopp friction model. They pointed out some of the advantages of this approach and showed how it could be used to create accurate and convincing displays of sliding friction, including pre-sliding displacement and stick-slip behaviors[6].

However, these studies of developing tactile displays use open-loop control in driving actuators of the display devices *i.e.* without any feedback mechanism for acquiring tactile perception information at the contact surface between a human finger pad and a display probe: While there are many studies using force and/or torque information as in [7], there has been no study in which actual contact state information concerning tactile perception was compared with the desired one so that it can be displayed by some compensation control. In this study, we propose a novel tactile device that has a feedback mechanism of displaying such information as to evoke accurate human tactile perception sensation by providing the device with such a feedback control mechanism as was mentioned above. We call this device a "tactile mirror". The term 'mirror' is used in the sense that the tactile perception sensation is reflected onto a human finger even if the contact state of the human finger surface is locally changed by disturbance. A part of a tactile which makes contact with a human fingertip is called a "pad". A tactile mirror is associated with conventional tactile displays, but there are critical points to be made that describe the difference between the two devices. The control structure of a tactile mirror is shown in **Figure 1**.

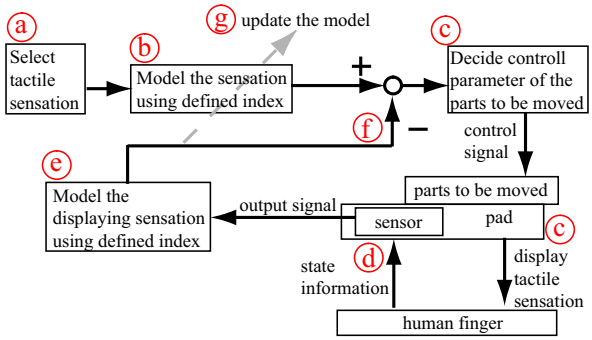

Figure 1: Control block diagram of a tactile mirror

The structure is composed of 7 blocks of phases to control a tactile mirror. First, **a)** a tactile perception sensa-

tion is determined which is desirably displayed. Next, **b)** modeling of the desired tactile perception sensation is performed. We refer to the data to be modeled as "tactile data", which do not contain force and/or torque information. In this phase, it is considered to be difficult to display complicated tactile perception sensation in the sense that multidimensional and sophisticated tactile image patterns cannot be easily converted to a tactile model of compressed data in lower dimensions. A surface condition that is contaminated by e.g. human sweating or changed by a mechanical displacement between a human pad and a display device probe can also be a serious problem. We consider, however, that the above problems can be solved by application of phase **g**. Next, **c)** control signals are computed using the modeled tactile data. Probes are actuated using the signals to display tactile perception sensation on a human finger. **d)** Sensors embedded in the pad detect the contact state on the surface of the fingertip. **e)** Actual tactile data are collected through the sensors. **f)** Tactile data in phase **b** and phase **e** are compared and an error of signals between the two channels is calculated. The error is fed back for the purpose of displaying tactile perception sensation more accurately. **g)** The tactile data obtained in phase **e** is used to update the model of tactile perception sensation at the same time. The difficult problem of displaying tactile perception sensation which can be modeled in the form of a multidimensional pattern converted to compressed tactile data in a lower dimension. If the conversion process does not operate appropriately, phase **g** updates the conversion process for a better mapping. The originality of this study is represented by the existence of phases **d** through **g**. There has been no report that had such a feedback mechanism about tactile perception sensation. In this paper, we stress that a tactile mirror which typically has phases from **d** to **f** is useful to display such a sophisticated tactile perception sensation in contrast to conventional display devices without any feedback control of contact state information.

2 Structure of a pad for static friction sensation

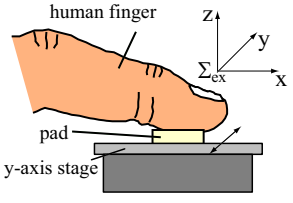

Figure 2: Schemetic of the human-pad(tactile mirror) system for static friction sensation

As was described in **section 1**, we set our target of tactile perception sensation as static friction sensation for the purpose of demonstrating the effectiveness of a tactile mirror. Johansson *et al.*[8] examined human static friction sensation. According to their suggestion, incipient slip has an important roll for the sensation. Later, several studies revealed that a robot hand grasps an object using such incipient slip information without dropping the object[9][10][11]. In this section, we introduce a control method for a tactile mirror paying our special attention to incipient slip.

Figure 2 is an overview of a pad for use of displaying static friction sensation. In this figure, a human fingertip contacts a pad with ridges in which vibrotactile sensory elements are embedded. The pad is fixed to a *y*-axis stage for generating relative displacements in the *y* direction.

2.1 Hardware structure of a pad

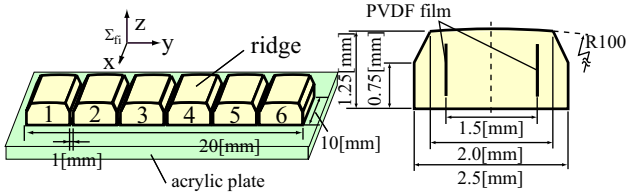

(a) structure of pad (b) section of a ridge located at an end

Figure 3: Structure of a pad

The structure of a pad is shown in **Figure 3(a)**. In this figure, a pad is composed of six ridges and the material for the ridges is silicone rubber(Shinetsu Silicone: KE12). There are 1mm distance between the two neighboring ridges. The bottom of the ridges are adhered to an acrylic plate. The reason of 1mm distance between the two is to prevent vibration occurred at one ridge from transmitting to the neighboring ones[12]. We label 1 through 6 to these ridges, which are shown in the figure. The pad is designed as having a macroscopically flat surface so that sufficient contact can be obtained between a human finger and the pad.

Details of one ridge are shown in **Figure 3(b)**. The curvature radius of the top surface is designed to be 100 mm: A local slip is spread slowly if the surface has smaller but nonzero curvature. Two strips of PVDF films(Kureha Chemical Industry Co.: KF Piezofilm 80μm) which are cut in the shape of 1×10 mm, and are embedded in one ridge as shown in this figure.

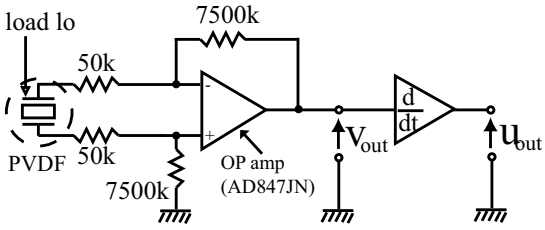

Figure 4: Circuit diagram of a PVDF circuit(PVDF transducer + amplifier + signal processing circuit)

A circuit system that converts the applied load *lo* to the voltage signals v_{out} and u_{out} is shown in **Figure 4**. Elec-

Table 1: Parameters of FEM analysis

Young's modulus	4.96 MPa
Poison's ratio	0.495
Mass density	1230 kg/m^3
Mechanical material	isotropic
FE Program	MARC(MSC.MARC2001)

tric charge is produced when PVDF film is given lo, and the current is converted to v_{out} through an OP amp circuit, and u_{out} is further produced by differentiating v_{out}. We call the overall signal processing circuit system a PVDF circuit. We definite the quantity *Gain* of either v_{out} or u_{out} in the following manner.

$$Gain(*_{out}) = 20 \log_{10} \left| \frac{*_{out}}{lo} \right| \qquad (* = v, u) \qquad (1)$$

The experimental result shows that the frequency characteristic of $Gain(v_{out})$ has a gradient of 18.5 dB/dec and that of $Gain(u_{out})$ is 38.5 dB/dec[12]. Howe *et al.* called this characteristic of PVDF stress rate[13]. We call v_{out} the stress rate and further u_{out} the 2nd-order stress rate, respectively.

3 Simulation results

In order to demonstrate the feasibility of a tactile mirror for static friction sensation, a contact analysis is conducted. Monitoring the stress distribution in the pad, signals generated from PVDF films which are embedded in the pad are estimated. The signals are used as inputs to an ANN(Artificial Neural Network) and the output signal is also analyzed.

3.1 Contact analysis result

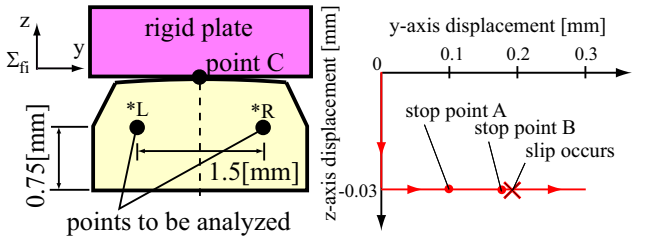

(a) analysis model (b) displacement of the point C on the bottom surface of rigid plate

Figure 5: Model of contact analysis

Using the model shown in **Figure 3(b)**, we analyzed the stress distribution when the pad made contact with a rigid plate and was moved until an incipient slip occurred. The analysis model is shown in **Figure 5(a)**. Points to be analyzed are marked as $*L$, $*R$ in the figure and the stress exerted at the points are defined as σ_{*L}, σ_{*R}, respectively. Material parameters in the model used are similar to those of a silicone rubber as specified in **Table 1**.

Under the condition that the bottom of the ridge in **Figure 5(a)** is fixed, the rigid plate is slid in the y direction in the simulation experiment. The schematic of displacement of the rigid plate is shown in **Figure 5(b)**. For the first 0.5 seconds, the rigid plate is moved downward at -0.06 mm/s speed in the z-axis direction. Second, the plate is moved horizontally at 0.2 mm/s speed in the y-axis direction until a slip occurs. It occurs at the point $\times$. Other experiments are conducted where the motion of the plate is stopped at the points **A** or **B**.

The result of a FEM analysis is shown in **Figure 6** where the rigid plate is moved in such a way as is described in **Figure 5(b)**, *i.e.* the plate stops neither at **A** nor **B**. The curves in **Figure 6** are the simulated results of the stress rate and the 2nd-order stress rate of the value of $\sigma_{*L} - \sigma_{*R}$. Let them be denoted as $\Delta\dot{\sigma}$ and $\Delta\ddot{\sigma}$, respectively. In the figure, the arrow pointing downward indicates the timing when a slip occurs at the contact surface. The result revealed the following two interesting points: First, the magnitude of $\Delta\dot{\sigma}$ increases gradually from 1.1 s to 1.4 s. Second, it decreases sharply and the magnitude of $\Delta\ddot{\sigma}$ oscillates when the slip occurs. We see that the slip can be detected by monitoring both $\Delta\dot{\sigma}$ and $\Delta\ddot{\sigma}$

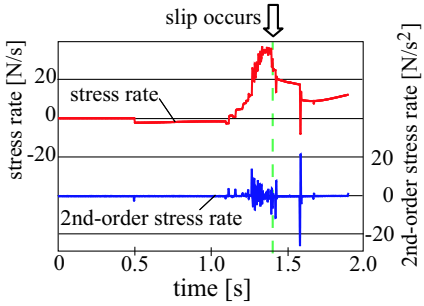

Figure 6: 1st and 2nd-order stress rate signals

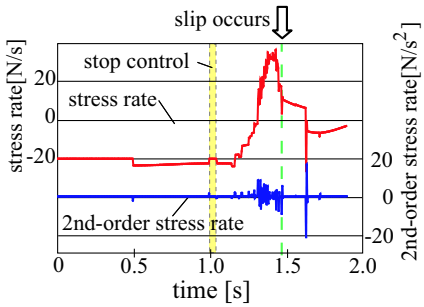

Figure 7: 1st and 2nd-order stress rate signals with stop control at point **A** in **Figure 5(b)**

Next, the result of a FEM analysis is shown in **Figure 7** where the rigid plate moves as is described in **Figure 5(b)** i.e. the plate stops only at **A**. In **Figure 7** as well, the arrow indicates the timing when a slip occurs at the contact surface. The rigid plate stops moving from t=1.0 s to 1.05 s, and starts moving at 1.05 s, again. In this case, $\Delta\dot{\sigma}$ is 0 while the plate is stopped, and a small impulse signal appears in $\Delta\ddot{\sigma}$ when the plate stops and restarts moving. There is little difference between the results in **Figure 6** and **Figure 7**.

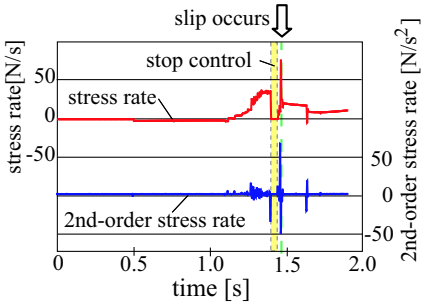

Figure 8: 1st and 2nd-order stress rate signals with stop control at point **B** in **Figure 5(b)**

Moreover, the result of another FEM analysis is shown in **Figure 8** where the rigid plate moves as is described in **Figure 5(b)** i.e. the plate stops only at **B**. In the figure, experimental data are represented when the plate stops moving from t=1.4 s to 1.45 s, and starts moving from 1.45 s, again. The $\Delta\dot{\sigma}$ curve shows that the magnitude of the differential stress rate increases gradually from 1.1 s to 1.4 s, and the magnitude becomes 0 when the plate stops moving. An impulse signal with large amplitude appears in the case of $\Delta\ddot{\sigma}$ when the plate stops. Both $\Delta\dot{\sigma}$ and $\Delta\ddot{\sigma}$ hit their peaked values when a slip occurs. It is important to distinguish the two signals, because the contact processes are entirely different from each other. Next section discusses a method for distinguishing the signals.

3.2 Method for judging slip occurrence

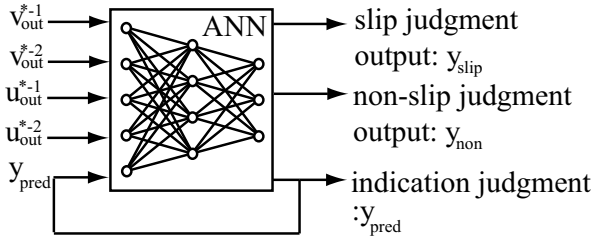

Figure 9: ANN architecture for slip judgment

Due to a potential necessity of increasing the number of sensor elements and a promise of expanding the proposed tactile mirror concept to other kinds of tactile perception sensation, ANN is used in the framework of our study, which can change the number of inputs and outputs with comparative ease. The architecture of the ANN for judging whether slip occurs is shown in **Figure 9**[12]. The ANN has five input and three output elements, and one hidden layer. The output neurons of ANN are:y_{slip} for judging slip occurs, y_{non} for judging no slip occurs, and y_{pred} for a prediction of slip occurrence. The input neurons to the ANN are v_{out}, u_{out} and y_{pred} where y_{pred} is a feedback element. The signals v_{out}^{*L} and v_{out}^{*R} are stress rates at $*L$ and $*R$ in **Figure 5(a)**, respectively, and the signals of u_{out}^{*L} and u_{out}^{*R} are 2nd-order stress rates at $*L$ and $*R$, respectively. Numerically, if the value of y_{slip} is larger than 0.8, we judge "a slip occurs on the ridge". Canepa *et al.* studied that the system presented is based on a ANN used to detect incipient slip[14]. The difference between their system and ours is whether a system includes a feedback element for memorizing the previous condition.

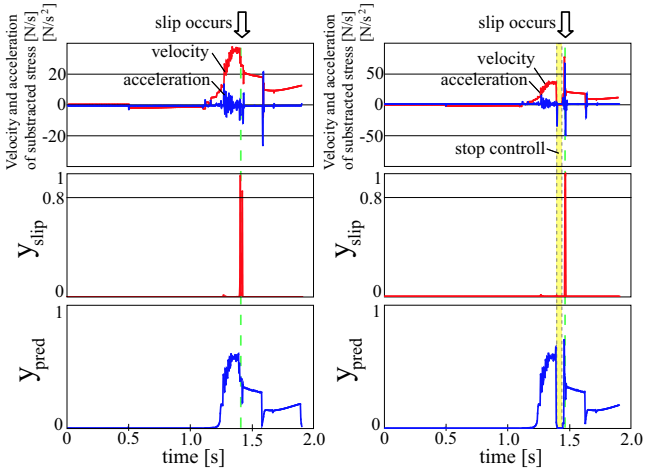

(a)result of using signal of Figure 6 (b)result of using signal of Figure 8

Figure 10: ANN result using FEM analysis signal of Figure 6 and Figure 8

The ANN is trained with the signals obtained from the FEM analyses described in **subsection 3.1**. Results of a slip judgment are shown in **Figure 10**. The figures in **Figure 10** (a) and (b) show judged results corresponding to the inputs in **Figure 6** and **Figure 8**, respectively. The top figures in **Figure 10** show the differential stress rate $\Delta\dot{\sigma}$ and 2nd-order stress rate $\Delta\ddot{\sigma}$ at $*L$ and $*R$, the middle figures show the slip signal y_{slip}, and the bottom figures show the slip prediction signal y_{pred}, respectively. We did not show the signal of judging there was no slip, y_{non}, because the result simply satisfies the relationship of $y_{non} = 1 - y_{slip}$. These results show that a correct judgment is made: When a slip occurs, the output signal y_{slip} grows over the threshold of 0.8. On the other hand, when the motion of the rigid plate is stopped, y_{slip} dose not overpasses the threshold. The results show that the ANN can judge only the case where a slip occurs. The output signal y_{pred} can make a judgment of slip prediction. Thus, when y_{pred} is given a certain magnitude and eventually, y_{slip} does not overpasses the threshold, the contact state is judged "a slip is likely to occur, but it dose not actually occur". Next, practical experiments using a set up with an actually developed tactile mirror are conducted by use of the previous described simulation results.

4 Experiments

Based on the simulation results in **section 3** which afford a technical prospect of monitoring the contact state transition from sticking to slipping through detection of an incipient slip, a tactile display is constructed to verify the effectiveness of a tactile mirror.

4.1 Experimental setup and method

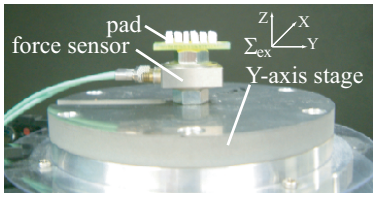

Figure 11: Experimental setup of a tactile mirror

A photograph of our experimental hardware setup is shown in **Figure 11**. A three axis force sensor(KISTLER: 9251A) is mounted on a *y*-axis stage(NIPPON THOMPSON CO.,LTD: CTS 125/125AE342), and a pad is fixed on the sensor. The force sensor is used to detect the *y* and *z* axis components of the force applied from a human finger through the pad.

Further, we set the following experimental procedure as follows: After placing the finger on the pad without any shearing force applied, a subject moves the finger in the *y*-direction as defined in **Figure 11** while keeping it in contact with the pad. For displaying the contact information without any slippage, the pad is necessary to be controlled to move in the direction with feedback information concerning where the finger is about to shift. And it is expected that y_{pred}, which is generated in advance of a slip and predicts its occurrence, plays the very role of such feedback information.

To demonstrate the usefulness of y_{pred}, we conducted the following two experiments. The first experiment employs open-loop control of the *y*-axis stage without feedback signal of y_{pred} and the second with y_{pred} feedback signal.

4.2 Experimental result

4.2.1 The experimental result of control without feedback element

An experimental result controlling the *y* axis stage without any y_{pred} feedback signal is shown in **Figure 12**. The top two curves are input signals of the ANN, v_{out} and u_{out}, the third and fourth curves are contact force components in the *y* and *z* directions, and bottom two curves are output signals from ANN; y_{slip} for judgment of slip occurrence and y_{pred} for the indication of slip occurrence. Again we do not show y_{non} because it always satisfies the relationship $y_{non} = 1 - y_{slip}$.

As is shown by the third and fourth curves, contact force is applied from the finger in the *y* and *z* directions, and y_{slip} reaches a peak value and overpasses a threshold at t=1.7 s meaning a slip occurs. Indeed, y_{pred} increases a little earlier than y_{slip} overpasses the threshold. We stress that the ANN system can detect the slip state of the contact surface, while the force sensor can not clearly capture that the slip occurs. The result shows that a local and small relative displacement of the finger on the contact surface cannot be detected by the force sensor. And we can conclude that controlling an actuator of a tactile display without any feedback information from the contact surface cannot appropriately display the desired contact state information of sticking.

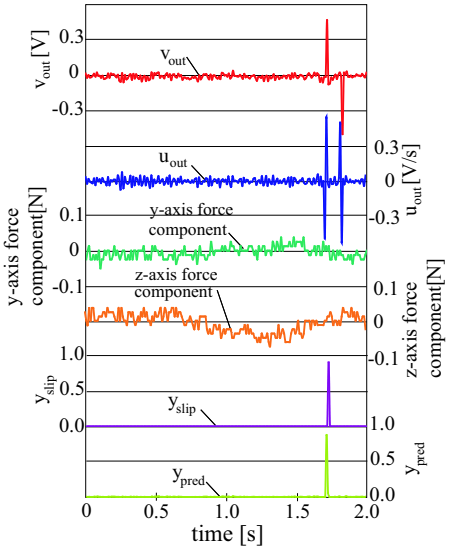

Figure 12: Experimental result without feedback control

4.2.2 Experimental result of control with feedback element

Experimental result of controlling the *y*-axis stage without any y_{pred} feedback signal is shown in **Figure 13**. The upper curves are defined the same as in **Figure 12** except for the bottom curve which shows displacement of the *y*-axis stage. The *y*-axis stage is controlled in such a way that the displacement is set in proportion to the amplitude of y_{pred} when it overpasses the threshold.

The experimental result shows that the *y*-axis stage is actually driven when y_{pred} increases and eventually slip does not occur, which is obvious from the fact that y_{slip} stays nearly zero. As is observed from the curve of the *y*-axis force component, the subject moves the finger randomly in the *y* direction in the experiment. However, the *y*-axis stage can track the finger movement. The result shows that the control mechanism with feedback of contact state information concerning tactile perception sensation performs effectively, and demonstrates that our proposal of a tactile mirror is useful.

This mechanism is considered to work effectively when a contact surface is subject to variation due for example to human sweating, or a loose mounting of a display device.

5 Conclusions

In this study, we stressed that there has been no study where contact state information concerning tactile perception sensation on a human finger pad side was fed back and compared with the desired information. From this

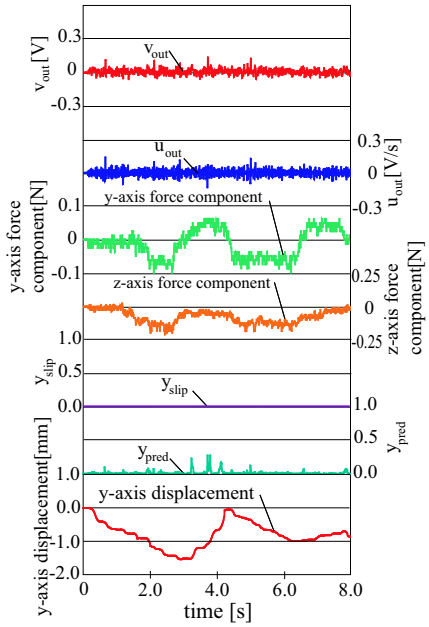

Figure 13: Experimental result with feedback control

viewpoint, we proposed a tactile perception sensation display with a feedback mechanism of monitoring the contact state information concerning tactile perception sensation of a human finger pad, and called it a tactile mirror in the study. We set our target of tactile perception sensation as static friction sensation for the purpose of demonstrating the effectiveness of a tactile mirror. And we introduced a control method for the tactile mirror paying our special attention detection of incipient slippage. For displaying incipient slips, we designed and manufactured a pad with 6 ridges, each having a pair of PVDF strips as sensors.

In order to demonstrate the feasibility of a tactile mirror for static friction sensation, a contact analysis was conducted. Monitoring the stress distribution in the pad, signals generated from PVDF films which were embedded in the pad are estimated. The signals are used as inputs ANN's and output signal is analyzed. For demonstrating the usefulness of y_{pred}, we conducted the following two experiments. The first experiment employed open-loop control of the y-axis stage without any feedback signal of y_{pred} and the second with a y_{pred} feedback signal. The result showed that the control mechanism with feedback of the contact state information concerning tactile perception sensation performed effectively, and demonstrated that our proposal of a tactile mirror was useful.

Future work of this study is to display other kinds of tactile perception sensation such as surface roughness sensation, by use of the concept of the tactile mirror.

Acknowledgments

We are indebted to Mr. Daisuke Yamada at Toyota Central Research and Development Laboratory Inc. for his helpful advice throughout this study. This study was supported by the Ministry of Education, Culture, Sports, Science and Technology under Grant-in-Aid for Scientific Research (B) No.10450161 and (B) No.15360139.

References

[1] Grigore C. Burdea, FORCE AND TOUCH FEEDBACK FOR VIRTUAL REALITY, pp.1–12 *JOHN WILEY & SONS, INC.*, 1996.

[2] F. Hosoe *et al.*, Development of Tactile Sensor Modelled after the Shearing Strain Perception Mechanism of theHuman Tactile Sense and Its Application *Transactions of the Society of Instrument and Control Engineers*, Vol.30, No.5 pp.577–583, 1994 (in Japanese).

[3] Dimitrios A. Kontarinis *et al.*, A Tactile Sensing and Display System for Teleoperated Manipulation, *IEEE International Conference on Robotics and Automation*, pp.641–646, 1995.

[4] L. Kruger, Pain and Touch, *Academic Press* pp.37–41, 1996.

[5] T. Debus *et al.*, MULTI-CHANNEL VIBROTACTILE DISPLAY FOR TELEOPERATED ASSEMBLY *IEEE International Conference on Robotics and Automation*, pp.592–597, 2002.

[6] C. Richard *et al.*, Friction modeling and display in haptic applications involving user performance, *Proceedings of the 2002 IEEE International Conference on Robotics & Automation*, pp.605–611, May 2002.

[7] S. Wang *et al.*, The role of Torque in Haptic Perception of Object Location in Virtual Enverонments, *Proceedings of the 11th International Symposium on Haptic Interfaces for Virtual Environment and Teleoperator Systems*, pp.302–309, 2003.

[8] R. S. Johansson *et al.*, Tactile sensory cording in the glabrous skin of the human hand, *Trends in Neuro-Sciences*,Vol.6, No.1, pp27–32, 1983.

[9] M. R. Trembly *et al.*, Estimating friction using incipient slip sensing during a manipulation task, *IEEE International conference on robotics and automation*, pp.429–434, 1993.

[10] J. S. Son *et al.*, A Tactile Sensor for Localizing Transient Events in Manipulation, *Proceedings of 1994 Int. Conf. on Robotics and Automation*, pp.471–476, 1994.

[11] D. Yamada *et al.*, Artificial Finger Skin having Ridges and Distributed Tactile Sensors used for Grasp Force Control, *Journal of Robotics and Mechatronics*,Vol.14, No.2, 2002.

[12] I. Fujimoto *et al.*, Development of Artificial Finger Skin to Detect Incipient Slip for Realization of Static Friction Sensation, *IEEE Conference on Multisensor Fusion and Integration for Intelligent Systems 2003*, pp.15–20, August 2003.

[13] R. D. Howe *et al.*, Dynamic tactile sensing: Perception of fine surface features with stress rate sensing, *IEEE transactions on robotics and automation*, Vol.9, No.2, pp.140–151, 1993.

[14] G. Canepa *et al.*, Detection of Incipient Object Slippage by Skin-Like Sensing and Neural Network Processing, *IEEE Transactions on Systems, Man, and Cybernetics-Part B: Cybernetics*, Vol.28, No.3, pp.348–356, 1998.